Engineering Science
2017; 2(4): 85-92
http://www.sciencepublishinggroup.com/j/es
doi: 10.11648/j.es.20170204.11

Experimental Study of Free Convection Inside Curvy Surfaces Porous Cavity

Ali Maseer Gati'a, Zena Khalifa Kadhim, Ahmad Kadhim Al-Shara

Mechanical Department, Engineering College, Wasitt University, Wasit, Iraq

Email address:
alimaseer10@gmail.com (A. M. Gati'a), profwasit@yahoo.com (Z. K. Kadhim), akm_alshara@yahoo.com (A. K. Al-Shara)

To cite this article:
Ali Maseer Gati'a, Zena Khalifa Kadhim, Ahmad Kadhim Al-Shara. Experimental Study of Free Convection Inside Curvy Surfaces Porous Cavity. *Engineering Science*. Vol. 2, No. 4, 2017, pp. 85-92. doi: 10.11648/j.es.20170204.11

Received: April 17, 2017; **Accepted**: April 27, 2017; **Published**: August 1, 2017

Abstract: An experimental investigation is performed in the present study to identify how can the porous medium behave inside a closed curvy porous cavity heated from below and compare the obtained results with the same numerical simulation model. The numerical model is simulated by ANSYS-CFX R15.0 under Darcy-Forchheimer model with neglecting the viscous dissipation. The work contains also measuring experimentally the permeability of the sand-silica which represents the solid matrix of the porous medium by using a special device made locally. The isotherms form and the temperature distribution on the interior sides of the walls are what explored in this experimental work. The final result leads to an acceptable convergence between these two models (numerical and experimental models). Also, the work gives a proof of the legality of Kozeny-Karman equation to estimate the permeability of the porous medium mathematically.

Keywords: Free Convection, Curvy Cavity, Porous Medium, Sand-Silica, Teflon, Darcy-Forchheimer Model

1. Introduction

This research is an integral part of our previous study which was published recently under the title (Numerical Study of Laminar Free Convection Heat Transfer Inside a Curvy Porous Cavity Heated From Below) [1]. In order to complete the main purpose of this numerical study about the effect of the PM on the convection HT inside a closed wavy cavity, we turned to the practical side via the use of two devices have been made locally here in this experimental work. One of them is designed according to the Heinemann's schema [2] which will be shown later to measure the permeability of the used PM (saturated silica-sand by water), whereas the other is designed to simulate only one numerical model practically. To identify the isotherms form it was used the Thermal Imager (thermal camera), while the thermocouples (K-type) were used to estimate the temperature distribution.

Silica is the name given to a group of minerals composed of silicon and oxygen, the two most abundant elements in the earth's crust. Silica is found commonly in the crystalline state and rarely in an amorphous state. It is composed of one atom of silicon and two atoms of oxygen resulting in the chemical formula (SiO_2). Sand consists of small grains or particles of mineral and rock fragments. Although these grains may be of any mineral composition, the dominant component of sand is the mineral quartz, which is composed of silica (silicon dioxide). Other components may include aluminum, feldspar and iron-bearing minerals. Sand with particularly high silica levels that is used for purposes other than construction is referred to as silica sand or industrial sand [3].

2. Numerical Chosen Model

The chosen numerical model is a two dimensional closed cavity filled with a PM. The side facing walls are sketched to be wavy sinusoidal walls. One of them (right one) is reflected about the vertical center line of the cavity as displayed in Figure 1. Number of waves per wall (N) is equal to (1) with wave's amplitude (a_d) equal to (0.15). As a boundary conditions, the facing side walls of the model are kept insulated to be adiabatic walls. The top surface is exposed to outside environment while the bottom surface is exposed to constant heat flux.

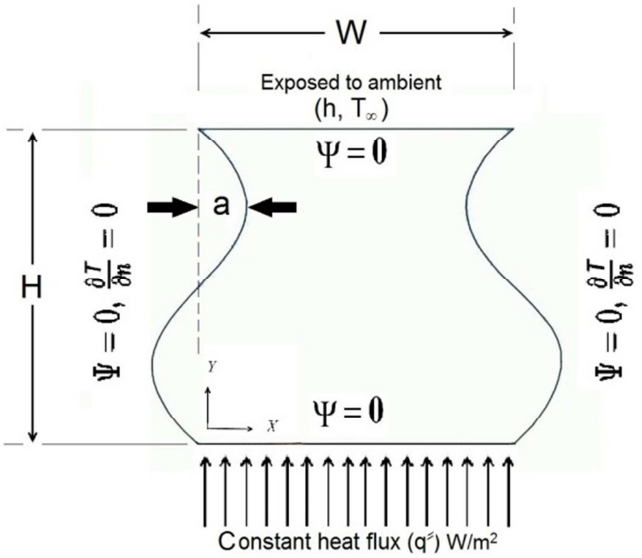

Figure 1. *Numerical chosen model and boundary conditions.*

3. Experimental Devices

As mentioned above, there are two main devices, one of them is used to measure the permeability of the chosen sand-silica and the other is used to simulate practically one selected numerical model only. Each one of them will be explained briefly in the following topics.

3.1. Permeability Measuring Device

This device was used to estimate the magnitude of the permeability of the silica-sand which is used in this study as a solid matrix of the PM. It had been designed according to the scheme of permeability measuring device that shown in Figure 2 which produced by Heinemann [2] with some amendments and it had been calibrated by comparing the result with Kozeny-Karman equation as will be shown below.

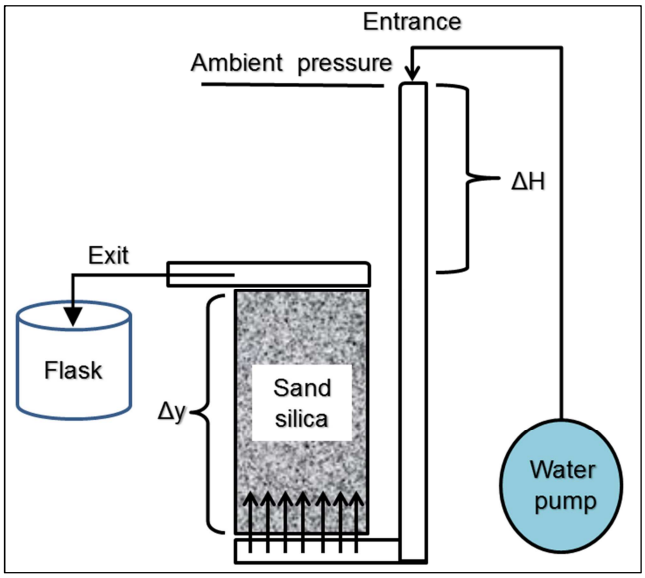

Figure 2. *Simple sketch to show operating of permeability measuring device.*

After filling the devise with silica-sand to (20) cm height, switch on the water pump to bring water up to the entrance (the funnel) which is on a (29) cm above the exit under ambient pressure. This distance represents the pressure difference (Δp) later in the calculations. Where many readings had been taken for time to fill a one-half litter flask then the average of these readings will be depending on to estimate finally the discharge amount.

To estimate the final value of the permeability of the chosen silica-sand, it was depending mainly on the following measured values of the water discharge and its temperature with the rest parameters as follows.

The measured water temperature (T_{wa}) = 25.5°C.

This temperature helps to find water density and its dynamic viscosity ➔

$$\rho_{wa} = 996.45 \text{ kg/m}^3$$

$$\mu_{wa} = 8.5856 * 10^{-4} \text{ kg/m.s} = 8.5856 * 10^{-1} \text{ cP (centipoise)}$$

Where; (1) kg/m.s = (1000) cP

The poise unit is used for the dynamic viscosity property in the system (centimeter–gram–second) of units.

The average time to fill the one-half litter flask (t) = 13 s.

This leads to estimate the average discharge ➔

$$Q_{wa} = ((0.5 \text{ lt}/1000) \text{ m}^3 / 13 \text{ s}) = 3.846154 * 10^{-5} \text{ m3/s} = 38.46154 \text{ cm}^3/\text{s}.$$

The water column height over the exit (ΔH) = 26.5 cm

This leads to compute the pressure difference ➔

$$\Delta p = \Delta H * \gamma_{wa} = \Delta H * \rho_{wa} * g = 2590.4212425 \text{ Pa} = 0.025565 \text{ atm}.$$

The cross sectional area (Ac) = $(\pi/4)*D^2 = (\pi/4)* (10 \text{ cm})^2 = 78.53982 \text{ cm}^2$. Flow distance (Δy) = 19.7 cm.

By using of the above measured amounts in the Darcy's law then the permeability will be estimated as follows ➔

$$K \text{ (1 Darcy)} = \{Q_{wa} \text{ (cm3/s)} * \mu_{wa} \text{ (cP)} * \Delta y \text{ (cm)}\} / \{Ac \text{ (cm2)} * \Delta p \text{ (atm)}\} = 323.996$$

This is the magnitude of the permeability in Darcy unit, which equals to ($3.1976 * 10^{-10}$ m^2), where (1 Darcy = $9.869233 * 10^{-13}$ m^2).

This value of the permeability of the silica-sand that used in this test is approximately the same value that can be gotten by using of the kozeny-karman equation which is used to estimate the permeability mathematically. This equation can be written in the general form as follows [4]:

$$K = \frac{\varepsilon^3}{2\tau.a_v^2.(1-\varepsilon)^2} \quad (1)$$

Where it can be released to the form:

$$K = \frac{phi^2 * D_{pa}^2 * \varepsilon^3}{150 * (1-\varepsilon)^2} \quad (2)$$

Where;

a_v: is the specific internal surface area of the medium (ratio of the exposed surface area to the solid volume).

τ: is the tortuosity of the medium (varies between 2 and 3). The tortuosity is commonly used to describe the diffusion in PM [5]. In the simplest mathematical method the tortuosity equals to ratio of the curve length to the distance between the ends of it [6].

Phi: is the sphericity of the beads or the shape factor (dimensionless).

For the silica-sand used in this test, taking phi=0.65, D_{pa}=0.001m, and ε=0.36 where the range of the sphericity of silica-sand beads can guess its value approximately between (0.75 – 0.65), then:

$$K = \frac{0.65^2 * 0.001^2 * 0.36^3}{150 * (1-0.36)^2} = 3.20836 * 10^{-10}\ m^2$$

3.2. Experimental Test Device

3.2.1. Manufacturing Steps

A numerical model has been chosen to simulate it practically which is taken from the reflected facing wall models as illustrated in Figure 3. It can be described by the following characteristics, where it have a (20) cm for height, one wave per height, (3) cm for wave wall amplitude, and aspect ratio equal to one.

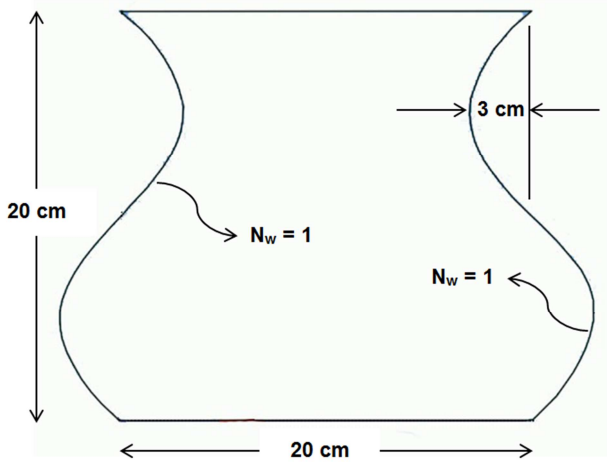

Figure 3. *A sketch of experimental model (front view).*

This model was simulated practically by using of a three different materials; Aluminum plate was used for top and bottom surfaces with (4) mm in thickness, A Teflon plate was used for walls and back side with (27) mm in thickness, and a transparent plastic plate (known as acrylic or acrylic glass) was used for front side with (5) mm in thickness. The two important properties of these last two materials are the sufficient resistance of heating beside the easiness of forming. The main steps to complete this work can be explained as follows:

(1) Manufacturing the wavy walls by using of electrical saw and finishing them by a milling machine. Then fixed them on the back side in their right position as shown in Figure 4 by using of a universal fast adhesive which is a set of activator and high viscosity cyanoacrylate adhesive called (Professional Soma Fix S663).

(2) Fixing thermocouples (K-type) in the wavy walls (three for each wall) by inserting each one of them into a hole of (6) mm in diameter which then is reduced to be (1-1.5) mm in diameter before reaching the end by (5) mm distance approximately. So that only the head of each thermocouple appears on the wavy side surface. To prevent water from entering these holes it was injected thermal silicone inside them which is a high temperature resistant RTV silicone used usually for fuel engines gasket. Figure 5 shows how this operation was achieved.

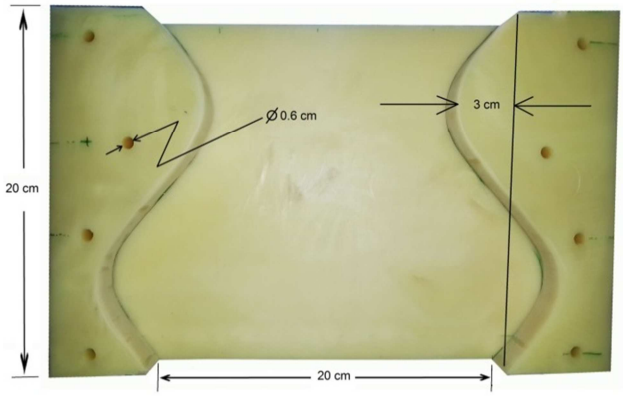

Figure 4. *Wavy walls and back side from Teflon.*

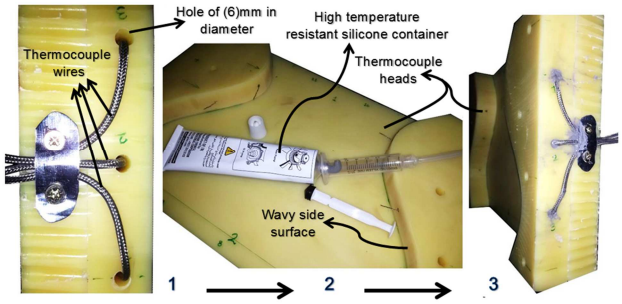

Figure 5. *Fixing thermocouples on wavy walls.*

(3) Closing the front side of the cavity with the transparent plastic plate by using of four bolts (5) mm in diameter on each side after painting the touching surface by thermal silicone to ensure perfect contact and prevent seepage of water as shown in Figure 6.

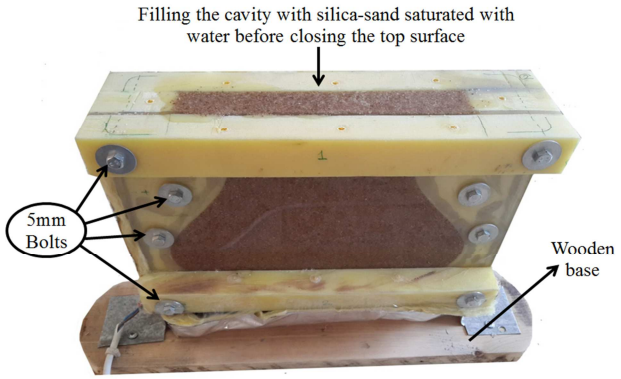

Figure 6. *Closing the front side of the cavity and filling it by PM.*

(4) Fixing the top and the bottom surfaces which are made from Aluminum plate (4) mm in thickness by using (8) expansion bolt screw with plastic anchors (6mm) for each one after painting touching surfaces by thermal silicone as shown in Figure 7. The important two steps before fixing the top surface were the adding of the chosen silica-sand and distilled water inside the cavity which represent the PM stuff and the fixing of thermocouples on each one of the top and bottom surfaces. This last step was achieved by using an adhesive epoxy putty (ALTECO Epo Putty A + B). It consists of two putties which are Resin (A) and Hardener (B), they are blended together by water and then the resulting paste is used in the place to be.

As an additional step to ensure that the porosity value of the chosen silica-sand is measured correctly, the cavity has been filled with water before adding the chosen silica-sand as much as represented the amount of the porosity from the overall size of the cavity. Where the overall size of the cavity was measured by ANSYS-CFX program. The result of this step was came fully confirmed the accuracy of the porosity value which have been estimated in the manner described in the paragraph 4.2.

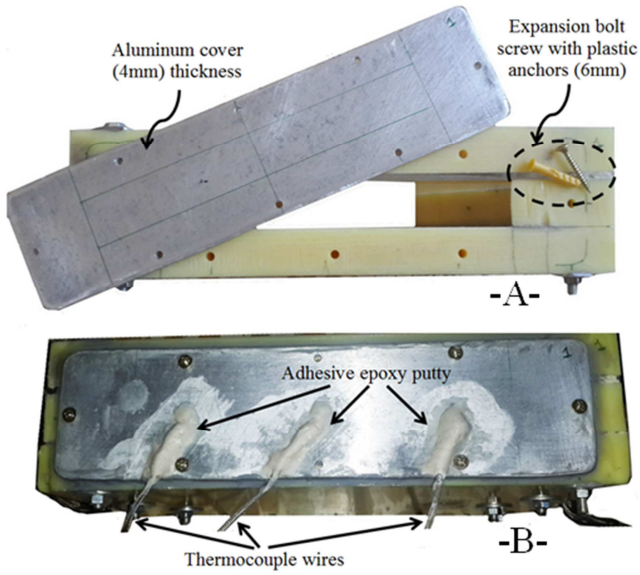

A. Before fixing. B. After fixing.

Figure 7. *Fixing the bottom cover and its thermocouples.*

(5) Fixing the Heater under the bottom surface, where it is a Halogen heater (400W/230V) comprises tungsten filaments in sealed quartz envelopes, mounted in front of a metal reflector as shown in Figure 8. It operates "at a higher temperature than Nichrome wire heaters but not as high as incandescent light bulbs, radiating primarily in the infrared spectrum. It converts up to 86% of their input power to radiant energy, losing the remainder to conductive and convective heat" [6].

The main reason of using this type of heaters is to ensure that the supplied heat flux will be distributed equally on all the bottom area of the cavity, where –as mentioned above- it converts up to 86% of their input power to radiant energy.

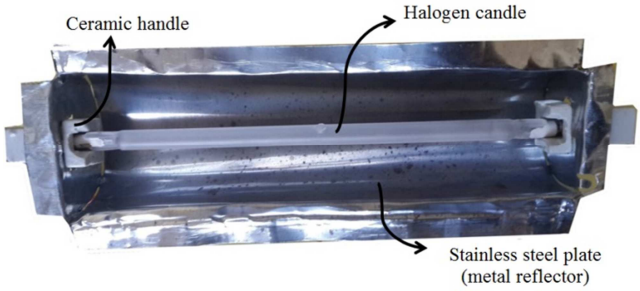

Figure 8. *Halogen Heater (400W/230V).*

3.2.2. Description of Some Used Materials

In this work there are two important materials that have been used, it is needed to be described here to complete this section as follows:

(i). Transparent Plastic Plate

It is a Poly (methyl methacrylate) (PMMA), also known as acrylic or acrylic glass as well as by the trade names plexiglas, Acrylite, Lucite, and Perspex, is a transparent thermoplastic often used in sheet form as a lightweight or shatter-resistant alternative to glass. The same material can be utilized as a casting resin, in inks and coatings, and has many other uses [7]. Table 1 shows its general properties.

Table 1. *General properties of acrylic glass [8].*

Melting point	160°C (433 K)
Thermal conductivity	0.17 - 0.2 W/(m·K)

(ii). Teflon (PTFE), Polytetrafluoroethylene

It is a synthetic fluoropolymer of tetrafluoroethylene that has numerous applications. The best known brand name of PTFE-based formulas is Teflon by Chemours. Chemours is a spin-off of DuPont Company, which discovered the compound in 1938 [9]. Table 2 shows its general properties.

Table 2. *General properties of Teflon [8].*

Melting point	327°C (600°K)
Thermal conductivity	0.25 W/(m·K)

3.2.3. Operating the Device

The test device has been operated inside an air-conditioning room to provide two important conditions; the first is a constant ambient temperature while the second is a stability in overall ambient HT coefficient. To get a constant heat flux from the Heater it was supplied a constant electrical current by using of a supply voltage regulator. The steady state was estimated by notice that the temperature at a two chosen points are not changed with time, where this was realized after passing (13) hours approximately as illustrated in Figure 9 below.

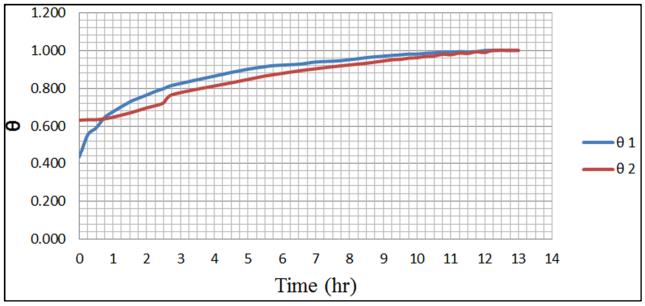

Each (θ) represents temperature in different place.

Figure 9. *Time for steady state (θ = reading temp./ final temp.).*

It is important to know the way of estimating the value of the overall ambient HT coefficient (h_a or OAHTC), where this done by three steps as follows ➔

(1) Calculating heat losses: there are -in general- three important directions needed to find the heat transfer losses from them. These directions are (front, back, and the sides), where:

q_{si} = the sides heat losses (W/m^2).

q_{fr} = the front heat losses (W/m^2).

q_{ba} = the back heat losses (W/m^2).

All of them can be calculated by using of the simple conduction heat transfer equation (Fourier equation). For example; a case that have (q_{in} = 2238 W/m2) the losses can be calculating as below:

$$q_{si} = - \Delta T_{si} / [\sum dx/\sum k]$$

$$= - \Delta Tsi [(1 / [(2*(\sum dx/3) / k_{teflon}) + (2*dx_{glasswool}/ k_{glasswool})])$$

$$= - 16.5 [(1 / [(0.12/ 0.25) + (0.01/ 0.04))$$

$$= - 22.6 \ W/m^2$$

Where; (ΔT_{si} = Average interior side temperature – T_a) and $\sum dx$ is the summation of the distance between inside points (thermocouples points) and the outside ($\sum dx$= 0.09 + 0.06 + 0.03=0.18) as illustrated in Figure 10.

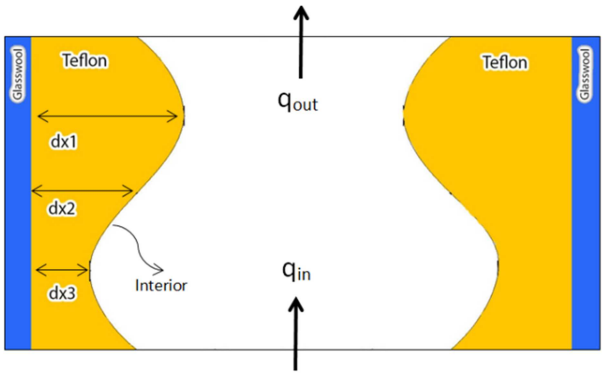

Figure 10. *Position of dx1, dx2, and dx3.*

$$q_{ba} = - \Delta T_{ba} / [\sum dx/\sum k]$$

$$= \Delta T_{ba} [(1 / [(dx4/ k_{teflon}) + (dx_{glasswool}/ k_{glasswool})])$$

$$= 16.5 [(1 / [(0.027/ 0.25) + (0.005/ 0.04)])$$

$$= - 70.8 \ W/m^2$$

Where; dx4 is the back side thickness (made from Teflon).

$$q_{fr} = - \Delta T_{fr} / [\sum dx/\sum k]$$

$$= \Delta T_{fr} [(1 / [(dx_{acrylicglass}/ k_{acrylicglass}) + (dx_{glasswool}/ k_{glasswool})])$$

$$= 16.5 [(1 / [(0.005/ 0.17) + (0.005/ 0.04)])$$

$$= - 107 \ W/m^2$$

Then;

$q_{tolosses}$ = Total heat losses

$$= q_{si} + q_{ba} + q_{fr} = 22.6 + 70.8 + 107 = 200.4 \ W/m^2$$

This means the percentage heat losses is (9%) approximately from the total supplied heat flux.

(2) Calculating the out heat transfer (q_{out}):

$$q_{in} = q_{out} + q_{tolosses}$$

$$2238 = q_{out} + 200.4$$

$$q_{out} = 2037.6 \ W/m^2$$

(3). Calculating the overall ambient heat transfer coefficient:

$$q_{out} = h_a . \Delta T_{top}$$

2037.6 = ha * 6 ➔ ha = 339.6 W/m^2. K (this large amount is due to the forced convection on the top surface of the device beside containing the other dissipation factors of heat like radiation).

Where; $\Delta T_{top} = T_{top} - T_a$

The procedure to operate the test device includes the following main steps:

(1) Setting up the device in an air-conditioning room nearing from a ceiling fan. This fan provided a speed of air vacillated between 0.33 to 3 m/s which measured by the Anemometer near the upper surface of the model.

(2). Balancing its situation with respect to the ground where y-axis of the device should be in a perpendicular direction to the ground.

(3). Supplying the specified electric power by the Slide Regulator to the Heater. Where the amount of both the supplied voltage and the electrical current were measured by the Ammeter.

(4). Recording the temperature for each specified points at every period of time. Each period was about 15 to 30 minutes until reaches the steady state where the temperature did not change with time. Also it was recorded the ambient temperature and the speed of air near the upper surface by using of the Hot Wire device. To estimate the heat losses, it was reading the temperature on the sides of devices which are defined above.

4. Results

4.1. Isotherm Lines

The isotherms form and the temperature distribution on

the interior side of the walls are what explored in this experimental work. To estimate the isotherms form it was used the Thermal Imager by focusing its lens towards the transparent side of the practical model when reaching the steady state then take a picture (thermal image). figures (11, 12, and 13) compare between the practical isotherms form and the theoretical one for the chosen model. As a result it can be said that there is a sketchy match between the two images.

Figure 11. *The transparent side of the practical model.*

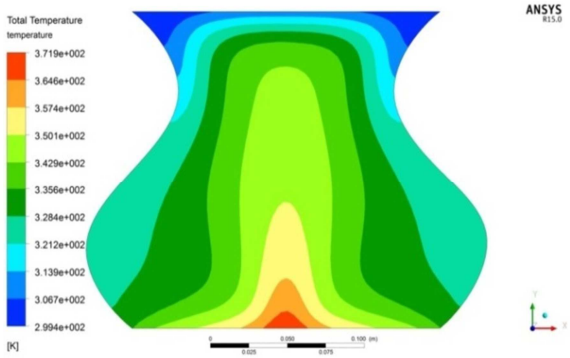

Figure 12. *Theoretical isotherms (state3).*

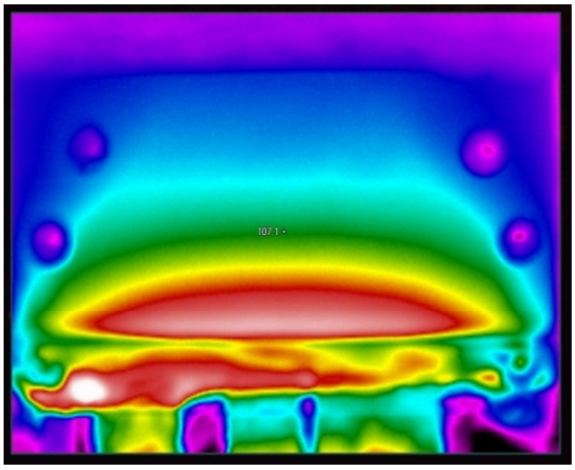

Figure 13. *Practical isotherms.*

4.2. Temperature Distribution

On the other hand, the temperature distribution on the interior sides of the cavity's walls is obtained by using a collection of thermocouples which were distributed on these sides as explained in Chapter Four. These eleven thermocouples were distributed as: three on each facing walls, three on the base, and two on the roof of the cavity and three amount of heat flux were supplied. Table 3 shows a comparison between experimental and corresponding theoretical results.

Table 3. *Experimental and theoretical results.*

Details	**State 1**		**State 2**		**State 3**	
	I_e=0.57 Amber. V_e=21.2 Volt. P_e=12.084 Watt (2238 W/m^2).		I_e=0.54 Amber V_e=16.9 Volt P_e=9.126 Watt (1538 W/m^2).		I_e=0.42 Amber. V_e=10 Volt. P_e=4.2 Watt (778 W/m^2).	
1. Results:						
Dimensionless temperature distribution						
Points	θ_{ex}	θ_{th}	θ_{ex}	θ_{th}	θ_{ex}	θ_{th}
1	0.668	0.798	0.721	0.822	0.820	0.879
2	0.630	0.794	0.685	0.818	0.811	0.874
3	0.585	0.768	0.649	0.794	0.786	0.852
4	0.665	0.798	0.721	0.822	0.822	0.878
5	0.622	0.794	0.685	0.818	0.814	0.874
6	0.585	0.767	0.649	0.793	0.786	0.852
7	0.993	0.916	0.997	0.925	0.994	0.947
8	1.000	1.000	1.000	1.000	1.000	1.000
9	0.975	0.917	0.985	0.926	0.989	0.947
10	0.482	0.714	0.555	0.752	0.680	0.829
11	0.479	0.714	0.551	0.751	0.682	0.828
θ = reading temperature /maximum reading temperature						
θ_{th} = theoretical dimensionless temperature distribution.						
θ_{ex} = experimental dimensionless temperature distribution.						
2. GNN						
	35.8	33.8	35.4	30.5	28.7	22.1
2. Ra						
	1157	1219	802	847	419	449

Figure 14 below shows the position of each point.

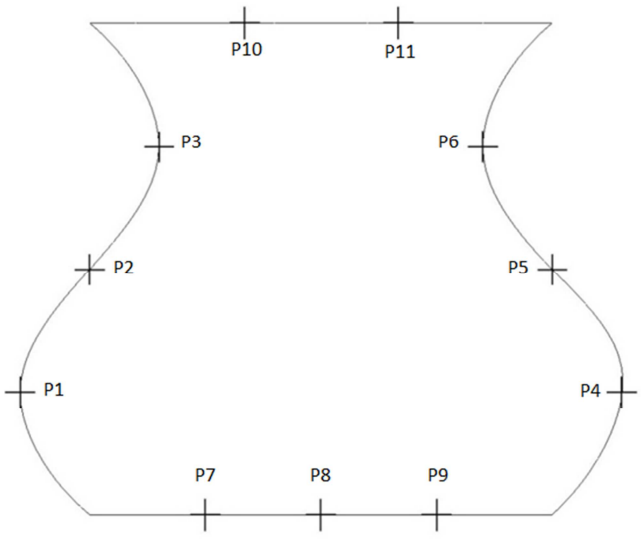

Figure 14. *Shows the position of each point.*

To complete the above comparison that shown in the previous table there are some important points which can be indicated as follows:

(1) To compute GNN for the practical model it is

depending on the obtainable temperatures, where the bulk temperature is estimated to be equal to [(Tp1 + Tp2 + Tp3 + Tp4 + Tp5 + Tp6 + Tp10 + Tp11)/8]. While the base temperature is taken to be equal to [(Tp7 + Tp8 + Tp9)/3].

(2) The experimental GNN is calculated with the available values. Where the bulk temperature is taken as the average value for the points (1, 2, 3, 4, 5, 6, 10, and 11), while the base temperature is taken as the average value for the points (7, 8, and 9).

(3) The temperature distribution for the side walls is graduated in descending from the lower point to the upper one for both the theoretical and the experimental ratios.

(4) For both distributions the maximum temperature value occurs in the middle of the base (P8).

(5) The mean percentage error in the temperature distribution of the experimental values with respect to the theoretical values is (14%) for all three states. This done by using of the standard percentage error formula which takes here the form (percentage error = $[(\theta_{th}-\theta_{ex})/\theta_{th}]*100$) and then it is taken the average as a mean (total) percentage error for all variables and all states.

(6) The mean percentage error for the GNN of the experimental values with respect to the theoretical values is (17.3%) for all three states.

(7) The points where the gap is greatest between the practical and theoretical results are (10 and 11) at the upper surface.

4.3. Mismatch Reasons

The mismatch between the experimental and theoretical results can be traced back to the following reasons:

(1) Losses in the supplied heat flux due to non-perfectly insulation.
(2) Roughness of the inside curvy walls.
(3) Instability of electricity beside the long time needed to reach the steady state.
(4) HT through walls by conduction from the base, which it was tried to prevent it by using of a material have a small value of thermal conductivity (Teflon and acrylic glass).
(5) Non-perfectly purity of used water.
(6) Errors in measurement devices.
(7) Missing of exactly properties of used materials.
(8) Blemishes in the solid matrix.

5. Conclusions

There is an important match between the numerical isotherm form and corresponding experimental isotherm form. This match gives additional strength to the legitimacy of the numerical research and the validity of the results obtained. Beside the match also of the temperature distribution on the interior side of the cavity walls.

The importance of this match comes as it proves the validity of the theoretical equations that used in the numerical simulation under Darcy-Forchheimer model.

The experimental results for heat transfer behavior inside the wavy closed porous cavity shows that the percentage approach with the corresponding numerical results is closed to be (85%) approximately. Also it is important to show that the permeability measuring device that designed and manufactured in the present work measures the permeability for the used silica-sand with percentage error equals to (0.34%) with respect to the kozeny-karman equation which measures the permeability mathematically.

Nomenclature

Symbol	Description	Symbol	Description
Ra	Modified Rayleigh number.	g	Gravitational acceleration (m/s^2).
Nu	Nusselt number.	A	Aspect ratio.
T	Temperature.	N	Number of waves per height.
k	Thermal conductivity (W/m. K).	a	Wave's amplitude (m).
K	Permeability (m^2).	a_d	Dimensionless wave's amplitude (a/H).
u	Velocity component at x-axis (m/s).	α	Thermal diffusivity (m^2/s).
ν	Velocity component at y-axis (m/s).	X	Stream function.
W	Cavity width (m).	q0 (HF)	Heat flux (W/m^2).
H	Cavity height (m).		
Subscript	Description	Subscript	Description
eff	Effective.	f	Fluid.
s	Solid.	a	Ambient.
Acronym			Description
PM			PM (media or medium).
HT			Heat transfer.
GNN			Global Nusselt number.
OAHTC			Overall ambient heat transfer coefficient (W/m^2. K).

References

[1] Ali Maseer Gati'a, Zena Khalifa Kadhim, and Ahmad Kadhim Al-Shara.'Numerical Study of Laminar Free Convection HT Inside a Curvy Porous Cavity Heated From Below'. Engineering Science journals. Vol. 2, Issue 2, April 2017.

[2] Zoltan E. HEINEMANN. 'Fluid Flow in Porous Media'. Textbook series, Volume 1, DI Barbara Schatz, October 2005.

[3] EUROSOIL, which is a member of IMA-Europe, the European Industrial Minerals Association, was founded in May 1991 as the official body representing the European industrial silica producers.

[4] Manmath N. Panda, and Larry W. Lake. 'Estimation of single-phase permeability from parameters of particle-size distribution'. AAPG Bull 1994; 78: 1028–39.

[5] Epstein, N. (1989), On tortuosity and the tortuosity factor in flow and diffusion through porous media, Chem. Eng. Sci., 44(3), 777– 779.

[6] ASHRAE Handbook - Heating, Ventilating, and Air-Conditioning Systems and Equipment (I-P Edition) American Society of Heating, Refrigerating and Air-Conditioning Engineers, Inc., 2008, Electronic ISBN 978-1-60119-795-5, table 2 page 15. 3.

[7] Hydrosight. "Acrylic vs. Polycarbonate: A quantitative and qualitative comparison" (http://www.hydrosight.com/acrylic-vs-polycarbonate-a-quantitative-and-qualitative-comparison).

[8] The free encyclopedia Wikipedia.

[9] Teflon™| Chemours Teflon™ Nonstick Coatings and Additives. www.chemours.com. Retrieved 2016-03-01. (https://www.chemours.com/Teflon/en_US)

[10] George S. Kell. 'Density, thermal expansivity, and compressibility of liquid water from 0 to 150 C: correlations and tables for atmospheric pressure and saturated reviewed and expressed on 1968 temperature scale'. journal of chemical and engineering data, Vol. 20, No. 1, 1975.